The Journal of Experimental Biology 205, 3925–3935 (2002)
Printed in Great Britain © The Company of Biologists Limited
JEB4496

Vision in the peafowl (Aves: *Pavo cristatus*)

Nathan S. Hart

Vision, Touch and Hearing Research Centre, School of Biomedical Sciences, The University of Queensland, Brisbane, QLD 4072, Australia

e-mail: n.hart@mailbox.uq.edu.au

Accepted 9 September 2002

Summary

The visual sense of the Indian blue-shouldered peafowl *Pavo cristatus* was investigated with respect to the spectral absorption characteristics of the retinal photoreceptors, the spectral transmittance of the ocular media and the topographic distribution of cells in the retinal ganglion cell layer. Microspectrophotometry revealed a single class of rod, four spectrally distinct types of single cone and a single class of double cone. In the case of the single cone types, which contained visual pigments with wavelengths of maximum absorbance (λ_{max}) at 424, 458, 505 and 567 nm, spectral filtering by the ocular media and the different cone oil droplets with which each visual pigment is associated gives predicted peak spectral sensitivities of 432, 477, 537 and 605 nm, respectively. Topographic analysis of retinal ganglion cell distribution revealed a large central area of increased cell density (at peak, 35,609 cells mm^{-2}) with a poorly defined visual streak extending nasally. The peafowl has a calculated maximum spatial resolution (visual acuity) in the lateral visual field of 20.6 cycles degrees^{-1}. These properties of the peafowl eye are discussed with respect to its visual ecology and are compared with those of other closely related species.

Key words: microspectrophotometry, colour vision, avian retina, visual pigment, cone oil droplet, photoreceptor, visual ecology, ganglion cell topography, ocular media, peafowl, *Pavo cristatus*.

Introduction

The peafowl *Pavo cristatus* is a lekking species and males (peacocks) do not provide resources for offspring. It is essential, therefore, for a female (peahen) to reliably assess the genetic 'fitness' of a given peacock prior to mating, so that she may adjust her reproductive investment proportionately. The elaborate train of the peacock represents at least one important indicator of male quality that is used by peahens in their assessment; peacocks with more elaborate trains have increased mating success (Petrie and Halliday, 1994), their offspring show improved growth and survival (Petrie, 1994) and peahens lay more eggs for peacocks with larger trains (Petrie and Williams, 1993).

Vision is the primary sense for most birds and, in addition to predator and prey detection, vision is obviously extremely important for intraspecific communication among peafowl, particularly in the assessment of male quality. However, almost nothing is known about their visual capabilities. This paper reports microspectrophotometric measurements of the spectral absorption characteristics of the visual pigments and oil droplets found in their retinal photoreceptors. These data are combined with measurements of the spectral transmittance of the ocular media to predict photoreceptor spectral sensitivities. Data on the topographic organization of the retinal ganglion cell layer are also presented.

Materials and methods

Adult (1 year old) Indian blue-shouldered peacocks *Pavo cristatus* L. obtained from commercial breeders were euthanased by approved humane methods (overdose of barbiturate anaesthetic). Birds for microspectrophotometric analysis were held in darkness for at least 1 h prior to sacrifice.

Microspectrophotometry

Following enucleation, retinal tissue was prepared for analysis using a microspectrophotometer (MSP) as described elsewhere (Hart et al., 1998, 1999, 2000a,c). Photoreceptors were mounted in a solution of 340 mosmol kg^{-1} phosphate-buffered saline (PBS; Oxoid, UK) diluted 1:3 with glycerol (BDH) and adjusted to pH 7.3 with 1 mol l^{-1} NaOH. Separate retinal preparations were made for the measurement of oil droplet absorptance spectra and these samples were mounted in pure glycerol.

Absorbance spectra (330–750 nm) of individual photoreceptor outer segments and oil droplets were measured using a computer-controlled, wavelength-scanning, single beam MSP (Hart et al., 1998). Sample and baseline scans were made from cellular and tissue-free regions of the preparation, respectively. The dimensions of the measuring beam were adjusted according to the size of the outer segment being measured, and varied from approximately 1 μm×1 μm for oil droplets and small cones to 2 μm×10 μm for rods. Rod outer

Table 1. *Characteristics of rod and cone photoreceptors in the retina of the peafowl (*Pavo cristatus*) measured using microspectrophotometry*

	Single cones				Double cones		Rods
Visual pigments	VS	SWS	MWS	LWS	Principal	Accessory	
Mean λ_{max} of pre-bleach absorbance spectra (nm)	423.7±2.3	458.0+2.0	504.6±1.9	566.8±1.1	567.3±1.5	566.2±0.9	503.7±0.9
λ_{max} of mean pre-bleach absorbance spectrum (nm)	423.3	457.6	504.5	566.2	567.1	566.3	503.7
Mean λ_{max} of difference spectra (nm)	420.6±4.8	464.6±2.8	510.1±2.2	570.3±2.8	568.2±2.9	566.3±1.2	506.2±0.7
λ_{max} of mean difference spectrum (nm)	421.6	463.9	509.7	569.6	567.6	566.7	506.2
Absorbance at λ_{max} of mean difference spectrum	0.004	0.013	0.017	0.017	0.017	0.014	0.040
Number of cells used in analysis	4	10	5	4	9	4	7

Oil droplets	T-type	C-type	Y-type	R-type	P-type (dorsal)	P-type (ventral)	A-type	
Mean λ_{cut} of absorptance spectra (nm)	<330	448.5±3.8	511.3±1.9	569.4±3.9	479.1±9.0	499.6±1.4	488.2±3.7	–
λ_{cut} of mean absorptance spectrum (nm)	<330	449.5	511.4	569.6	482.5	499.6	489.9	–
Mean λ_{mid} of absorptance spectra (nm)	<330	462.1±3.3	525.4±2.3	591.9±4.3	498.8±5.0	513.6±1.4	500.9±3.4	–
λ_{mid} of mean absorptance spectrum (nm)	<330	462.7	525.6	592.4	500.4	513.6	502.3	–
Mean diameter (μm)	3.2±0.8	3.6±0.2	3.6±0.3	3.8±0.3	3.8±0.4	4.0±0.3	1.5±0.5	–
Mean maximum transverse absorptance	<0.01	0.88±0.02	0.90±0.02	0.92±0.02	0.48±0.11	0.90±0.03	0.36±0.23	–
Number of oil droplets used in analysis	8	9	28	29	9	22	6	–

Values are means ± 1 S.D.

λ_{max}, wavelength of maximum absorbance; λ_{cut}, wavelength of the intercept at the value of maximum measured absorptance by the line tangent to the oil droplet absorptance curve at half maximum measured absorptance; λ_{mid}, wavelength of half maximum measured absorptance (Lipetz, 1984).

Avian rods do not contain oil droplets. T-, C-, Y-, R-, P- and A-type oil droplets are located in the VS, SWS, MWS and LWS single cones and the principal and accessory members of the double cone pair, respectively. Spectra of P-type oil droplets vary considerably between the dorsal and ventral retina.

See list of abbreviations and text for more details.

segments were fairly robust, measuring approximately 15 μm long and 3–3.5 μm in diameter. Cone outer segments, on the other hand, were usually folded over, or otherwise distorted, so it was difficult to estimate transverse pathlength or outer segment length. For this reason, specific absorbance per μm of cone outer segment was not calculated and the absorbance at the λ_{max} of the mean difference spectrum was given instead (Table 1).

Data were recorded at each odd wavelength on the 'downward' long- to short-wavelength spectral pass and at each interleaved even wavelength on the 'upward' short- to long-wavelength spectral pass. Each scan (either sample or baseline) consisted of two downward and two upward spectral passes in alternate succession; spectral passes of the same direction were averaged together. To reduce the effects of in-scan bleaching, only one sample scan was made of each outer segment, but this was combined with two separate baseline scans. Averaging the two absorbance spectra obtained in this way improved the signal-to-noise ratio of the spectra used to determine the wavelengths of maximum absorbance (λ_{max}) of the visual pigments (Bowmaker et al., 1997). Following the 'pre-bleach' scans, outer segments were bleached with full spectrum 'white' light from the monochromator for 5 min and an identical number of sample and baseline scans made subsequently. The 'post-bleach' average spectrum thus created was deducted from the pre-bleach average to produce a bleaching difference spectrum for each outer segment.

To establish visual pigment-oil droplet pairings, the spectral absorptance of the oil droplet associated with the outer segment (if present) was also measured. A single sample scan was made of each droplet and combined with a single baseline scan. Each scan consisted of only one downward and one upward spectral pass, which were not averaged together. Higher quality oil droplet spectra, showing less evidence of by-passing light (Lipetz, 1984), were obtained from the retinal preparations mounted in pure glycerol, which reduces wavelength-dependent scattering of the MSP measuring beam (Hart et al., 1999).

Analysis of visual pigment absorbance spectra

Baseline and sample data were converted to absorbance values at 1 nm intervals. Upward and downward scans were averaged together by fitting a weighted (delta function) three-point running average (Hart et al., 2000c). Pre- and postbleach absorbance spectra were then normalized to the peak and long-wavelength offset absorbances determined by fitting a variable-point unweighted running average to the data. Following the method of MacNichol (1986), a regression line was fitted to the normalized absorbance data between 30% and 70% of the normalized maximum absorbance. The regression equation was used to predict the wavelength of maximum

absorbance (λ_{max}) following the methods of Govardovskii et al. (2000). Scans from each photoreceptor type that satisfied established selection criteria (Hart et al., 1999; Levine and MacNichol, 1985) were averaged and reanalysed. Criteria were relaxed for SWS single cones (see Abbreviations), as it was impossible to obtain spectra that did not show at least some distortion of the short wavelength limb.

Analysis of oil droplet absorptance spectra

Sample and baseline data were converted into absorptance and normalized to the maximum and long-wavelength offset absorptances obtained by fitting an unweighted 13-point running average to the data (Hart et al., 1998). Oil droplet absorptance spectra are described by their λ_{cut}, which is the wavelength of the intercept at the value of maximum measured absorptance by the line tangent to the oil droplet absorptance curve at half maximum measured absorptance (Lipetz, 1984). For comparison with other studies (e.g. Partridge, 1989), the wavelength corresponding to half maximum measured absorptance (λ_{mid}) is also given (Lipetz, 1984).

Spectrophotometry of ocular media

Absorbance measurements of the cornea, aqueous humour, lens and vitreous humour from one bird were made over the range 200–800 nm using a Shimadzu UV2101 PC UV-VIS scanning spectrophotometer fitted with a Shimadzu ISR-260 integrating sphere assembly to reduce the effects of light scattering by the tissue samples. Because the eyes were too big to measure in their entirety, the ocular media were measured separately (Hart et al., 1999), and pathlengths were determined from measurements of a radially sectioned frozen eye (see below).

The lens was dissected away from the anterior segment of the eye and placed in a rectangular aluminium insert, designed to fit inside a standard (10 mm pathlength) quartz cuvette, in which a 7.3 mm diameter hole (the same diameter as the lens) had been drilled to coincide with the measuring beam of the spectrophotometer and in which the lens could be positioned in its normal orientation relative to the incident light. Thin plastic rings were lodged inside the insert hole in front of and behind the lens to prevent movement. The cornea was excised from the sclera and measured whilst sandwiched between two stainless steel mesh inserts inside a standard cuvette. Both cornea and lens were bathed in 340 mosmol kg^{-1} PBS, which was also placed in the identical inserts and cuvettes used as reference samples.

Vitreous humour was removed from the vitreal body and placed in the hole (4.5 mm diameter) of an aluminium cuvette insert identical to that used to measure lenticular absorbance. The vitreous, which is a highly viscous gel, was trimmed in the insert to give a pathlength of exactly 10 mm. Aqueous humour was removed from the anterior chamber, using a hypodermic syringe, and measured in a 200 µl, 10 mm pathlength quartz cuvette. Both humours were measured relative to distilled water.

The spectrophotometer performed a single spectral pass from 800 nm to 200 nm, recording absorbance at 1 nm intervals. The spectral full width at half maximum bandwidth of the monochromator used by the spectrophotometer was set at 5 nm to maximise light transmission and signal-to-noise ratio, which are otherwise low when using an integrating sphere.

Determination of optical pathlengths in the peafowl eye

Pathlengths of the aqueous and vitreous humours along the optic axis were estimated from scaled photographs of a frozen eye, hemisected sagittally using a cryostat. Eyes were frozen at –20°C and attached to the chuck of a motor driven microtome using OCT embedding compound (BDH). The eye was orientated such that sections made by the cryostat were parallel to the optic axis, and 10 µm sections were made at –20°C until the edge of the lens was visible. Photographs of the eye, and a scale ruler positioned adjacent to the cut face of the eyeball, were then taken after every 10 sections, approximately 0.1 mm intervals. The negatives obtained were projected with a magnification of approximately ×13 using a photographic enlarger and the pathlengths of the aqueous and vitreous calculated according to the scale ruler.

Expansion of the eye upon freezing has a negligible effect on the calculated pathlengths. If the eye is modeled as a sphere 21 mm in diameter (mean of axial and equatorial diameters), and it is assumed that the thermal expansivity of the aqueous and vitreous humours is similar to that of water, the total pathlength along the optic axis of the frozen eye would only be approximately 35 µm longer than at body temperature. This increase in pathlength due to freezing (approximately 0.2%) was less than the likely error in estimating the pathlength by measuring an enlarged photograph (±1.4–5.3%).

Retinal whole-mount preparation and analysis

The retina and vitreous of one eye was removed intact by dissection in 340 mosmol kg^{-1} PBS and the pigment epithelium adhering to the photoreceptor layer removed gently with a fine paintbrush. The free-floating retina was fixed for 30 min in 4% paraformaldehyde in 0.1 mol kg^{-1} phosphate buffer (pH 7.2) and then washed in PBS. The retina was cleared of vitreous and floated onto a gelatinised slide (Fol's mounting medium; Stone, 1981) with the ganglion cell layer uppermost. Relieving cuts were made at the periphery to enable the retina to lie flat, and the preparation flooded with fresh Fol's medium. The retina was covered with Whatman #50 filter paper soaked in 16% paraformaldehyde in 0.1 mol l^{-1} phosphate buffer. A large coverslip was placed on top of the filter paper and a small weight (85 g) applied to the coverslip to ensure that the retina fixed flat to the slide (modified from Moroney and Pettigrew, 1987). The preparation was stored in a moist chamber for 24 h, after which the weight was removed and the slide washed in distilled water. The retina was then allowed to dry on the slide slowly in a moist chamber over several days to avoid cracking.

The retina was defatted in xylene (two changes, each 30 min), rehydrated through a descending alcohol series (100%, 95%, 70%, 50% ethanol and then distilled water for 10 min each) and stained for Nissl substance in an aqueous solution of 0.05% Cresyl Violet titrated to pH 4.3 with glacial acetic acid for 25 min. After rinsing in distilled water, the stained retina was passed through 70% and 95% ethanol (30 s

each) before immersion in a differentiation solution (95% ethanol titrated to pH 3.6 with glacial acetic acid) for a further 30 s. The retina was finally dehydrated (95% ethanol, followed by two changes of 100% ethanol, each 30 s) and cleared in xylene before mounting in DPX (Aldrich).

Counts of Cresyl Violet-stained neurons in the ganglion cell layer were made at 1 mm intervals (0.5 mm intervals in the regions of highest density) across the retina using a Zeiss Axioplan microscope at a total magnification of ×1000. Initially, all cell bodies that stained for Nissl substance were counted, with the exception of the very darkly stained spindle-shaped glial cells associated with the optic nerve fibre layer.

The retina was then recounted in an attempt to distinguish ganglion cells from putative displaced amacrine cells in the ganglion cell layer. Ganglion cells were identified by their relatively larger size, polygonal cell bodies, abundant darkly staining cytoplasm containing clumped Nissl substance and paler staining nucleus; putative displaced amacrines were identified by their smaller oval or teardrop-shaped perikarya with little cytoplasm and relatively darker, homogeneous staining (Chen and Naito, 1999; Ehrlich, 1981; Hayes, 1984; Stone, 1981), see Fig. 1. Like ganglion cells, the soma size of displaced amacrine cells decreases towards the centre of the retina (Hayes, 1984). Consequently, in the central retina of the peafowl – where Nissl-stained cells were present at high densities, ganglion cell somata were increasingly, circular or oval in shape, and somata overlapped considerably – a population of relatively smaller neurons morphologically similar to the putative displace amacrines in the more peripheral regions could still be distinguished. Nevertheless, it is always possible that some displaced amacrines were counted as ganglion cells and small ganglion cells in the central retina were wrongly classified as displaced amacrine cells. Therefore, both sets of count data are presented.

Cell densities were plotted on a ×10 scale drawing of the retina traced onto graph paper using the stage micrometer reading. Points of isodensity were calculated by linear interpolation and the line segments connecting these were smoothed by eye (Wathey and Pettigrew, 1989) to give the contour lines shown in Fig. 6A,B. Shrinkage of the retina during preparation was estimated by measuring the change in area of a chicken *Gallus gallus domesticus* retina prepared in an identical fashion to that of the peafowl. Retinal outlines were traced from enlarged (×16) scaled photographs of a whole-mounted chicken retina taken before and after fixation and after Nissl-staining. The outlines and scale bars were digitised using a flat-bed scanner connected to a microcomputer and retinal areas calculated using Image Tool V3.00 for Microsoft Windows (University of Texas Health Service Centre, San Antonio, USA). Shrinkage of the free-floating retina during fixation was 2.3%. The retina shrunk a further 8.7% throughout the Nissl-staining proceedure, although shrinkage occurred predominantly at the retinal periphery. However, cell counts were not corrected for shrinkage because, in the case of the peafowl, a total retinal shrinkage of 11% would decrease the estimate of maximum spatial resolution by less than 1 cycle degree^{-1}.

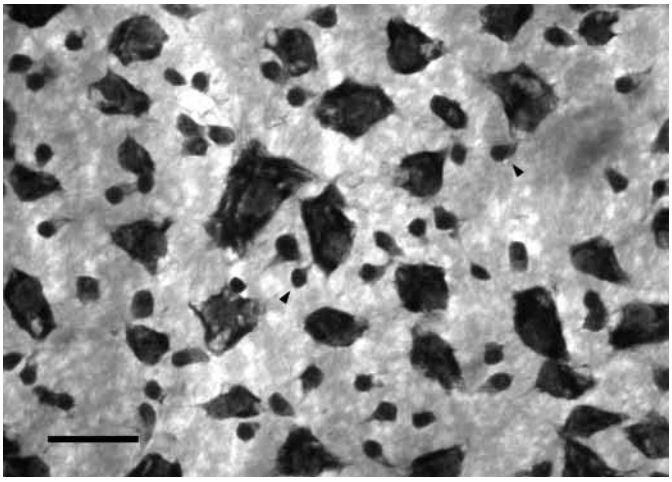

Fig. 1. Photomicrograph of Nissl-stained cells in the retinal ganglion cell layer of the peafowl *Pavo cristatus*. Ganglion cells are characterised by their large polygonal cell bodies, darkly staining abundant cytoplasm and pale staining nucleus. Putative displaced amacrine cells in the ganglion cell layer (such as those indicated by arrowheads) are usually round, oval or teardrop shaped and much smaller than the ganglion cells. Scale bar, 20 μm.

Estimating visual resolution

Peak cell density data from counts of the whole-mounted retina were used to estimate the theoretical resolution limits for the peafowl eye. The posterior nodal distance (PND) of the eye was estimated by multiplying its axial length (measured from an enlarged scaled photograph) by 0.60. This ratio is identical to that measured empirically for the chicken (Schaeffel and Howland, 1988), starling *Sturnus vulgaris* (Martin, 1986) and blackbird *Turdus merula* (Donner, 1951), and similar to the mean for diurnal eyes (0.67) from a variety of vertebrate species calculated by Pettigrew et al. (1988).

The distance d subtended by one degree on the retina was determined from the calculated PND and the formula:

$$d = (2\pi\mathrm{PND})/360\,. \quad (1)$$

Assuming that ganglion cells are the limiting factor for spatial resolution and that they are packed in a hexagonal array, the mean cell-to-cell spacing S was calculated using the formula:

$$S^2 = 2/(D\sqrt{3})\,, \quad (2)$$

where D is the density of ganglion cells per mm^2. The maximum spatial (Nyquist) frequency v of a sinusoidal grating resolvable by this array was then defined (Snyder and Miller, 1977) as:

$$v = 1/(S\sqrt{3})\,. \quad (3)$$

This value was multiplied by d to give spatial resolution in cycles per degree.

Results

Microspectrophotometry

Microspectrophotometric data for visual pigments (Figs 2,

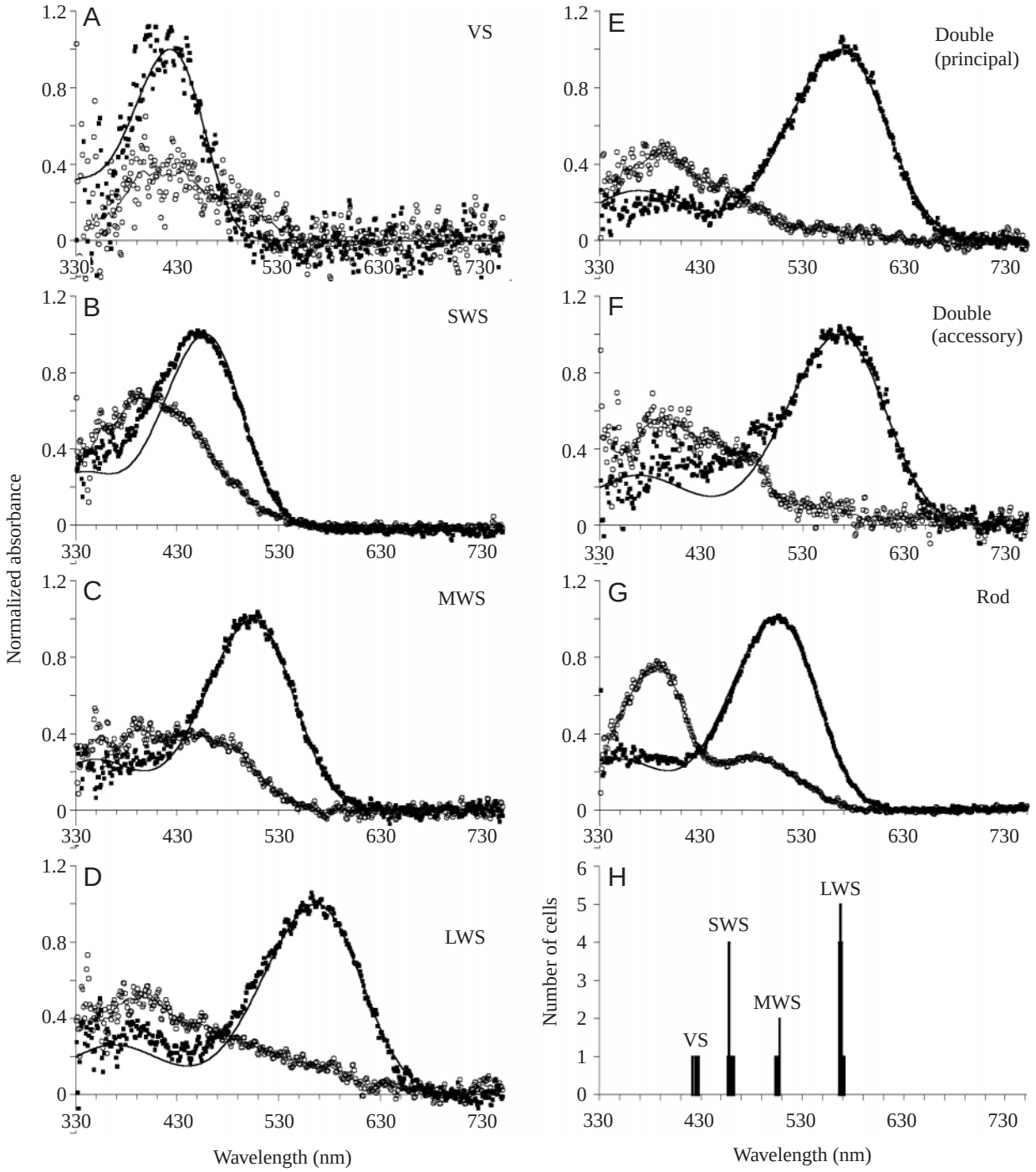

Fig. 2. (A–G) Normalized pre-bleach (filled squares) and post-bleach (open circles) absorbance spectra of visual pigments in the peafowl *Pavo cristatus*. Pre-bleach spectra are overlayed with best-fitted rhodopsin templates (bold line; Govardovskii et al., 2000). Post-bleach spectra are fitted with a variable point running average (thin line). (H) The spectral distribution of the wavelengths of maximum absorbance (λ_{max}) of the individual cone visual pigment absorbance spectra used to create the mean spectra. The group labeled as LWS in the histogram includes LWS single cones and both the principal and accessory members of the LWS double cone pair. VS, SWS, MWS and LWS refer to violet, short wavelength, medium wavelength and long wavelength sensitive single cones, respectively.

3) and oil droplets (Fig. 4) are summarized in Table 1. The peafowl retina contains five different types of vitamin A_1-based visual pigment (on the basis of their similarity to rhodopsin, rather than porphyropsin, visual pigment templates) in seven different types of photoreceptor cell. Rods contained a medium wavelength ('green') sensitive (MWS) visual pigment with a λ_{max} at 504 nm. There were four spectrally distinct types of single cone. Firstly, a violet sensitive (VS)

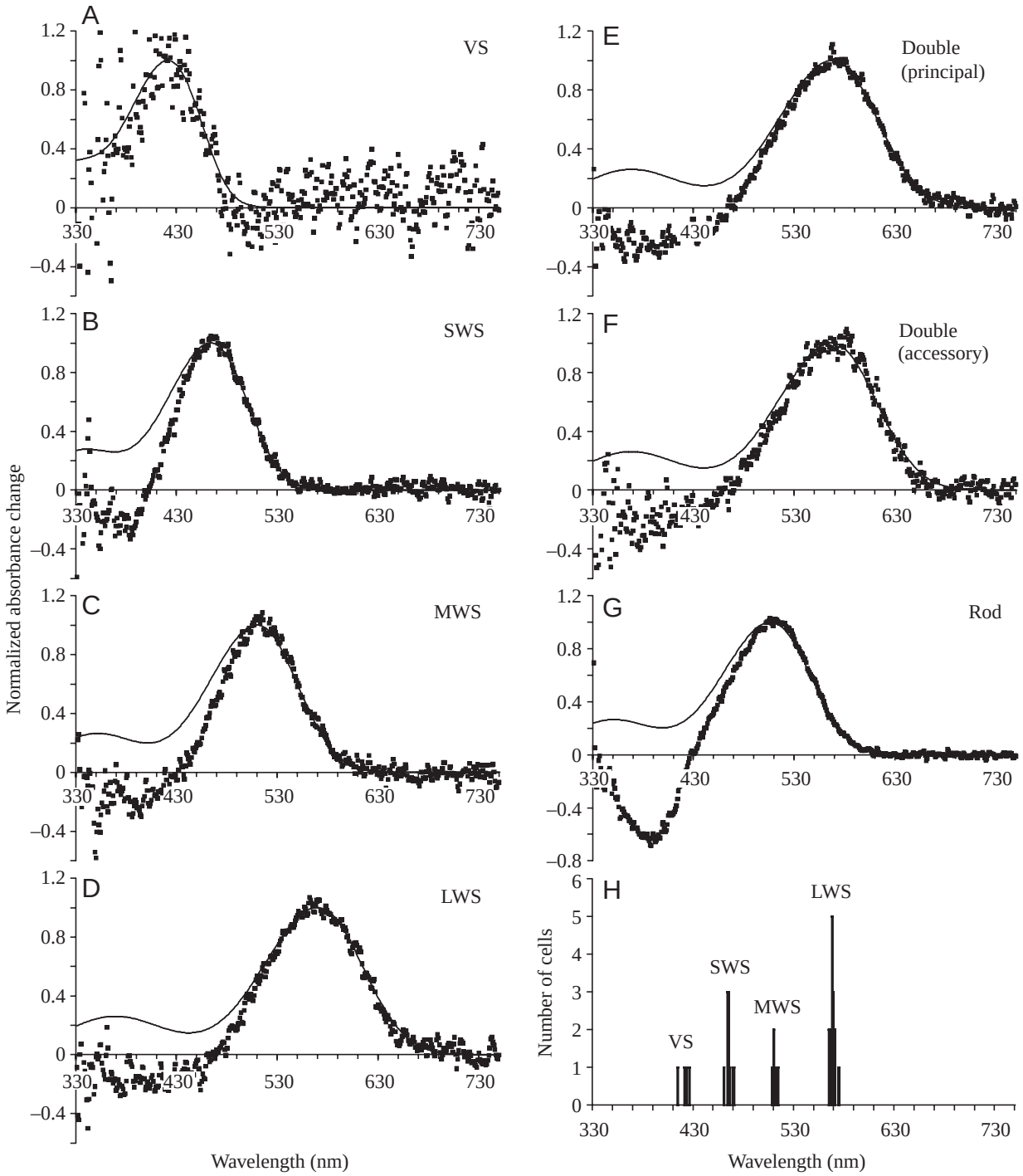

Fig. 3. (A–G) Normalized mean difference spectra (symbols) and best-fitted rhodopsin visual pigment templates (lines) for the visual pigments in the peafowl *Pavo cristatus*. Difference spectra represent the change in absorbance of the outer segment on bleaching with white light (see text for details). (H) The spectral distribution of the wavelengths of maximum absorbance (λ_{max}) of the individual cone visual pigment difference spectra use to create the mean spectra. For further details see legend for Fig. 2.

type with a visual pigment λ_{max} at 424 nm and a transparent T-type oil droplet that showed no detectable absorptance between 330 and 750 nm. Secondly, a short wavelength ('blue') sensitive (SWS) type with a 458 nm λ_{max} visual pigment and a colourless/pale green C-type oil droplet with a λ_{cut} at 449 nm. Thirdly, a MWS type with a 505 nm λ_{max} visual pigment and a golden yellow Y-type oil droplet with a λ_{cut} at 511 nm. Finally, the fourth type of single cone was maximally sensitive to long ('red') wavelengths (LWS) and contained a 567 nm λ_{max} visual pigment and a red R-type oil droplet with a λ_{cut} at 596 nm.

Good quality absorbance spectra were obtained for almost

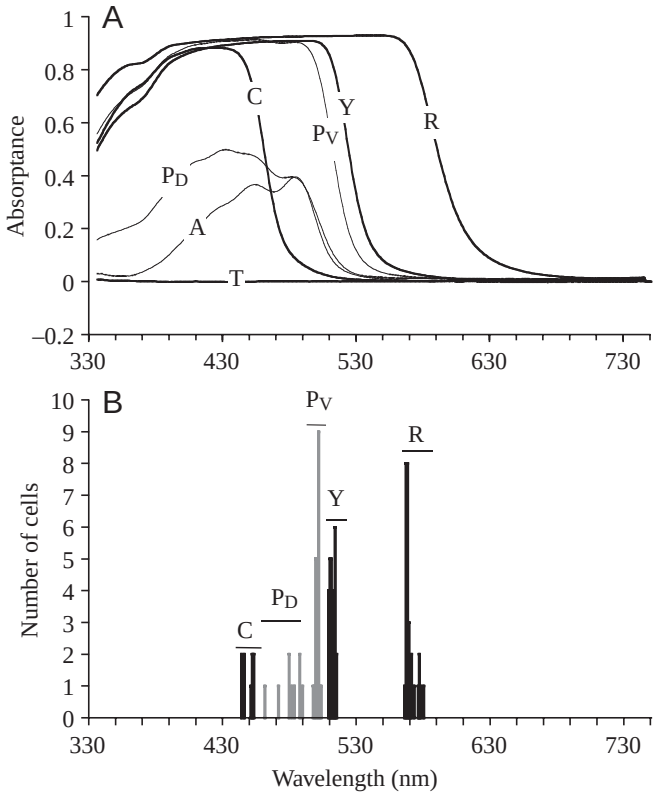

Fig. 4. Mean absorptance spectra (A) of oil droplets found in the single and double cone photoreceptors of the peafowl *Pavo cristatus*. T, C, Y, R, P and A refer to the T-type ('transparent'), C-type ('colourless'), Y-type ('yellow'), R-type ('red'), P-type ('principal/pale') and A-type ('accessory') oil droplets found in the VS, SWS, MWS and LWS single cones and the principal and accessory members of the double cone pair, respectively. Subscripts D and V refer to whether the P-type oil droplets were measured in the dorsal or ventral retina, respectively, as noticeable differences in the spectra obtained from these two retinal regions were observed. (B) The spectral distribution of the cut-off wavelengths (λ_{cut}) of the C-, Y-, R- and P-type oil droplets used to create the mean spectra. Note that P-type oil droplets measured in the ventral retina have a λ_{cut} at longer wavelengths than those measured in the dorsal retina.

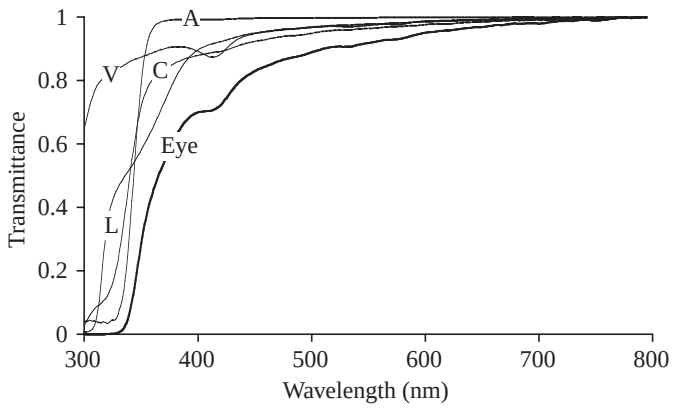

Fig. 5. Transmittance of the individual components and combined ocular media of the peafowl *Pavo cristatus*. C, L, A and V refer to the cornea, lens and aqueous and vitreous humours, respectively. Spectral transmittance measurements of small portions of aqueous and vitreous humours were adjusted for *in vivo* pathlengths along the optic axis using a frozen sectioned eye (see text for details). Adjusted transmittances for the aqueous and vitreous were summed with measurements of the intact cornea and lens to give the transmittance along the optic axis of the combined pre-retinal ocular media (Eye). The wavelength of 0.5 transmittance $\lambda T_{0.5}$ was 365 nm.

all of the photoreceptors, but it can be seen in Fig. 2 that the mean absorbance spectrum of the SWS visual pigment is distorted on the short wavelength limb, having a slightly higher absorbance at each wavelength than would be expected on the basis of a visual pigment template (Govardovskii et al., 2000). This is most probably due to the build up of stable photoproducts in the outer segment as a result of in-scan bleaching, similar to those that can be seen in the post-bleach absorbance spectra of all the cone types (Fig. 2). Consequently, the λ_{max} values calculated for the SWS visual pigment may be less reliable than the other cone types. However, the λ_{max} is predicted from the absorbance values on the long wavelength limb, and the λ_{max} values calculated from the difference spectra shown (Fig. 3, Table 1) are not very different from those calculated from the pre-bleach spectra.

Both the principal and accessory members of the double cone pair contain a LWS visual pigment that is spectrally identical to the one found in the LWS single cones (Figs 2, 3). In the dorsal retina, the P-type oil droplets in the principal member had a mean λ_{cut} at 479 nm and appeared pale green under bright field illumination. In the ventral retina, however, P-type oil droplets had λ_{cut} at longer wavelengths (mean λ_{cut} 497 nm) and appeared pale yellow. The pale greenish-yellow A-type oil droplet in the accessory member had a λ_{cut} at 488 nm. The oil droplets of both members of the double cone pair are located nearer the sclera than the single cone oil droplets. Of the single cones, the C- and T-type oil droplets of the SWS and VS cones, respectively, are located closer to the vitreous than the R- and Y-type oil droplets.

Spectrophotometry of ocular media and calculated pathlengths

Calculated pathlengths of the aqueous and vitreous humours along the optic axis of the peafowl eye were 3.2 mm and 10.6 mm, respectively, for an eye measuring 19.8 mm in axial length (lens axial thickness 4.3 mm). Measured absorbances for the aqueous and vitreous (10 mm pathlength; see above) were scaled appropriately, summed with the absorbance data for the cornea and lens, and the combined absorbance converted to transmittance for display (Fig. 5). The wavelength of 0.5 transmittance ($\lambda T_{0.5}$) was at 365 nm and the ocular media ceased to transmit light below approximately 330 nm.

Retinal ganglion cell distribution

The isodensity contour maps of both total cell counts (Fig. 6A) and presumptive ganglion cells only (Fig. 6B) are similar and reveal a prominent area centralis in the central

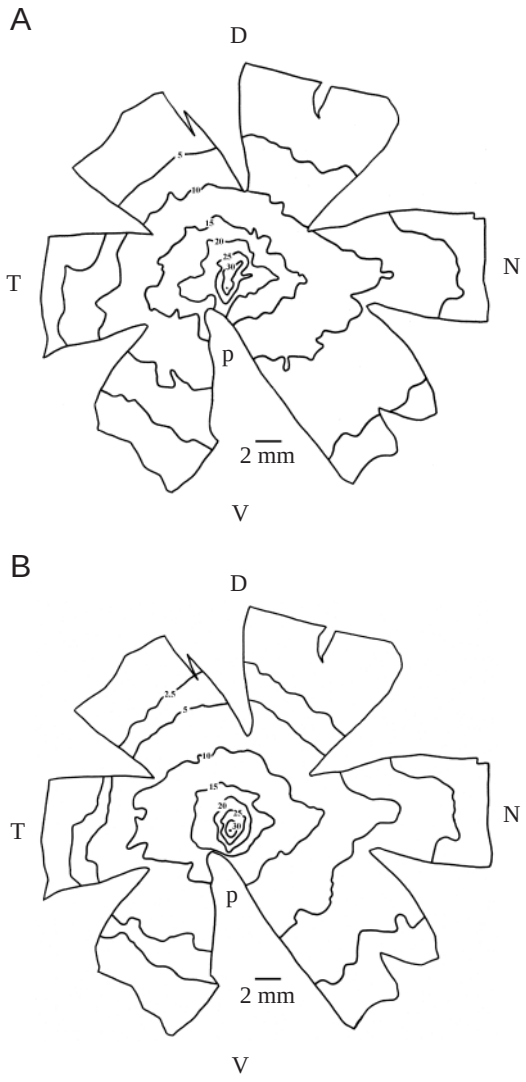

Fig. 6. (A,B). Topography of cells in the ganglion cell layer of the peafowl retina (right eye). (A) All cells excluding glia; (B) Presumptive ganglion cells only (see Fig. 1 and text for details of criteria used). In both cases a prominent area centralis, with the possibility of a visual streak of high density extending from the area centralis towards the nasal retina, is indicated. Lines represent isodensity contours; numbers represent $\times 10^3$ cells mm^{-2}. The black dot at the centre of the retina represents the location of the highest density count obtained (35.6×10^3 ganglion cells mm^{-2} in B). D, V, T and N refer to the dorsal, ventral, temporal and nasal aspects, respectively. The approximate location of the pecten (p) is also shown.

retina, approximately 2 mm nasal and dorsal to the top of the pecten. The density of presumptive ganglion cells (Fig. 6B) in the ganglion cell layer decreased concentrically from a peak of approximately 35,609 cells mm^{-2} in the area centralis to a minimum of 816 cells mm^{-2} at the dorsal periphery. Closer examination reveals a poorly defined horizontal visual streak of high cell density extending nasally from the area centralis.

Resolution limit

The unfixed eye from which the counted retina was taken had a measured axial length of 19.4 mm and an estimated PND of 11.6 mm (see Materials and methods). Thus, one degree of visual angle subtended 0.20 mm on the retina. The Nyquist frequencies calculated from the highest cell density counts for all cells in the ganglion cell layer (37 649 cells mm^{-2}) and presumptive ganglion cells only (35 609 cell mm^{-2}) were 21.2 cycles degrees^{-1} and 20.6 cycles degrees^{-1}, respectively (not corrected for retinal shrinkage).

Discussion

Microspectrophotometric data

The spectral characteristics of the visual pigments and oil droplets in the retinal photoreceptors of the Indian blue-shouldered peafowl *Pavo cristatus* are very similar to those described in the other galliform species studied to date: the domestic chicken *Gallus gallus* (Bowmaker et al., 1997), domestic turkey *Meleagris gallopavo* (Hart et al., 1999) and Japanese quail *Coturnix coturnix japonica* (Bowmaker et al., 1993) (for a review, see Hart, 2001b). They also resemble those measured in the mallard duck *Anas platyrhynchos* (Jane and Bowmaker, 1988), which belongs to the order Anseriformes that is thought to be closely related phylogenetically to the Galliformes (Sibley and Monroe, 1990). Galliform and anseriform photoreceptors are characterised by a VS (λ_{max} 415–426 nm) rather than UVS (λ_{max} 362–373 nm) visual pigment in the single cone containing a transparent T-type oil droplet.

The possession of a VS visual pigment is correlated with a shift in SWS visual pigment λ_{max} to longer wavelengths relative to SWS visual pigments found in birds with UVS visual pigments (Hart et al., 2000a) and increased spectral filtering (higher transverse absorptance and λ_{cut} at longer wavelengths) in the C-type oil droplet with which the SWS visual pigment is associated (Bowmaker et al., 1997). Both of these factors will serve to reduce the overlap between the spectral sensitivities of the VS and SWS cone classes (Fig. 7), potentially improving colour discrimination and colour constancy under a variety of illumination conditions (Barlow, 1982; Govardovskii, 1983; Vorobyev et al., 2001, 1998).

As well as reducing the overlap between adjacent spectral classes, spectral filtering by the oil droplets in the SWS, MWS and LWS single cones shifts the peak sensitivity of each cone to a longer wavelength than the λ_{max} of the visual pigment it contains; in the case of the peafowl, to 477, 537 and 605 nm, respectively (Figs 7, 8). The peak sensitivity of the VS cone is shifted to about 432 nm because of increasing absorption at short wavelengths by the ocular media. Excluding double cones, the potentially tetrachromatic colour vision system of the peafowl has, therefore, three spectral loci of maximal wavelength discrimination, where the cone spectral sensitivities overlap (Delius and Emmerton, 1979; Jacobs, 1981), at approximately 462, 517 and 576 nm (Figs 7 and 8).

The visual systems of birds have presumably evolved primarily for finding food and avoiding enemies (Lythgoe,

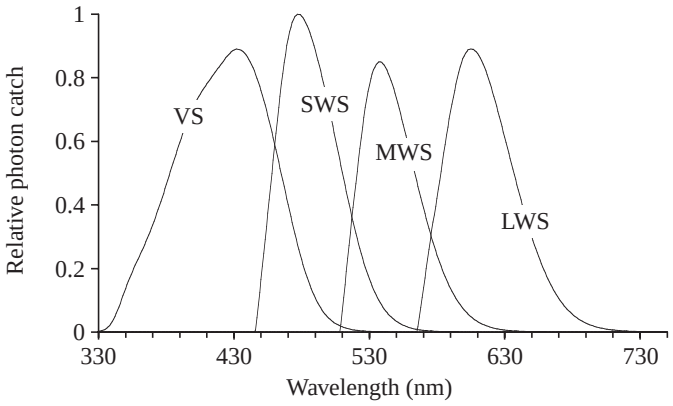

Fig. 7. Calculated relative photon catches for each of the single cone types in the retina of the peafowl *Pavo cristatus*. Visual pigment spectral absorptance was modeled using mathematical templates of the appropriate λ_{max} (Govardovskii et al., 2000). The outer segments of all single cones were assumed to be 16 μm long (as for the chicken, Morris and Shorey, 1967) and contain a visual pigment with an end-on specific absorbance of 0.015 μm^{-1} (Bowmaker, 1977). The calculated spectral absorptance of each visual pigment was multiplied by the spectral transmittance of the combined ocular media (Eye in Fig. 4), the spectral transmittance (1-absorptance), and cross-sectional area (diameters from Table 1) of the relevant oil droplet, and normalized to the SWS cone.

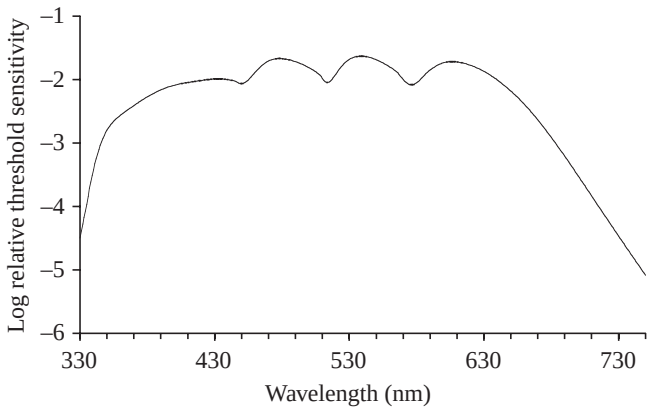

Fig. 8. Predicted relative threshold spectral sensitivity for the potentially tetrachromatic colour vision system of the peafowl *Pavo cristatus*. The model used is that given by Vorobyev and Osorio (1998) and assumes that thresholds are determined by photoreceptor noise, that noise in a given colour channel is proportional to the reciprocal of the square root of the relative proportion of that cone type in the retina, and that the level of noise in a cone is independent of spectral sensitivity. VS, SWS, MWS and LWS single cones were assumed to be present in the ratio 1:1.9:2.2:2.1, respectively (Hart, 2001a). Spectral sensitivities for the different cone types were those presented in Fig. 7.

1979); both the spectral characteristics of their photoreceptors (Hart et al., 2000a) and variations in the relative abundance of the different cone types across their retinae (Hart, 2001a; Partridge, 1989) appear to reflect diet, feeding behaviour, habitat and even phylogeny rather than intra- or interspecific variations in body coloration. It seems likely, therefore, that rather than driving the evolution of avian colour vision, conspicuous and sexually attractive coloration would take advantage of pre-existing visual mechanisms (Lythgoe, 1979). In the case of the peafowl, we might predict that the plumage colours designed to predict male quality would have peaks in reflectance spectra overlapping those regions of maximal wavelength discrimination. The plumage of the male peafowl is characterised by blue and green feathers that may well have reflectance peaks in these spectral regions, but such speculation must be tested using objective measurements of plumage coloration (Bennett et al., 1994). It may also be productive to compare plumage reflectance spectra between males that differ in their mating success to determine any chromatic component to the assessment of male quality. Although only males were used in this study there is no precedent to expect the visual systems of the males and females to differ in the spectral characteristics or the relative abundance of their photoreceptors (e.g. Hart et al., 2000a,b, 1998).

Microspectrophotometric data, together with estimates of the relative abundance of the different cone types in the retina, can be used to predict the relative threshold spectral sensitivity of a visual system (Vorobyev and Osorio, 1998). Such estimates have been shown to match behaviourally measured threshold spectral sensitivities well for di-, tri- and tetrachromatic colour vision systems operating under photopic light levels. The model of Vorobyev and Osorio (1998) assumes that photoreceptor noise limits discrimination and that noise in a given receptor colour channel is proportional to the reciprocal of the square root of the relative proportion of a given receptor type in the retina. I have applied this model to the potentially tetrachromatic visual system of the peafowl (Fig. 8), using photoreceptor proportion data described elsewhere (Hart, 2001a) and the predicted quantum catches displayed in Fig. 7. Unfortunately, there are as yet no behavioural data to compare the model against.

Spectrophotometry of ocular media

As with other species that possess a VS visual pigment (wavelength of 0.5 transmittance, $\lambda T_{0.5}$, 358–380 nm), the ocular media of the peafowl ($\lambda T_{0.5}$=365 nm; Fig. 4) transmit fewer short wavelengths than species with UVS visual pigments ($\lambda T_{0.5}$=316–343 nm; for a review, see Hart, 2001b). Consequently, while the VS visual pigment confers considerable sensitivity to near ultraviolet wavelengths (at least in the mallard duck; Parrish et al., 1981), it is clear that the visual systems of species with a VS visual pigment are functioning over a narrower range of short wavelengths than those with a UVS visual pigment. However, it is not yet known if the spectral characteristics of the ocular media determine the λ_{max} of the visual pigment in the single cone containing the T-type oil droplet or *vice versa* (Hart, 2001b).

Topography of the retinal ganglion cell layer

It is generally acknowledged that the topographic organisation of the retina represents an evolutionary adaptation

to the habitat and life style of a given species, both in terms of ganglion cell (e.g. Collin and Pettigrew, 1989; Hughes, 1977) and photoreceptor (e.g. Ahnelt and Kolb, 2000; Hart, 2001a; Partridge, 1989) distribution. The macroscopic topography of the avian retina has been studied extensively using ophthalmoscopy (e.g. Moroney and Pettigrew, 1987; Wood, 1917) and, to a lesser extent, using anatomical techniques (e.g. Binggeli and Paule, 1969; Budnik et al., 1984; Chen and Naito, 1999; Hayes et al., 1991; Hayes and Brooke, 1990; Inzunza et al., 1991; Wathey and Pettigrew, 1989), and a variety of organizations are evident (for reviews, see Martin, 1985; Meyer, 1977).

The Indian peafowl has a single, large, centrally located area of increased ganglion cell density, the area centralis. In this respect it differs from both the domestic chicken and the Japanese quail *Coturnix coturnix japonica*, to which it is closely related phylogenetically (Sibley and Monroe, 1990), both of which have an area of increased ganglion cell density in the dorso–temporal retina (area dorsalis) in addition to the area centralis (Budnik et al., 1984; Chen and Naito, 1999). The presence of only one area in the peafowl retina may reflect differences in feeding behaviour of this species compared to the chicken and quail. In the pigeon *Columba livia*, and presumably other species with similar retinal specialisations, the area dorsalis projects into a region of visual space in front of and just below the beak, which corresponds to the region of binocular overlap of the left and right visual fields, and is thought to facilitate pecking at and grasping nearby objects, especially food (Nalbach et al., 1993). The red jungle fowl *Gallus gallus*, which is the ancestor of the domestic chicken, and the Japanese quail, both feed predominantly on the seeds of grasses and weeds and occasionally small invertebrates (ants, beetles, termites). The peafowl, however, prefers slightly more substantial items, including many green crops, insects, small reptiles, mammals and even small snakes, berries, drupes and figs (del Hoyo et al., 1994). These larger visual targets may obviate the need for a specialized region of high spatial resolution in the dorso–temporal retina. It is also possible that the peafowl has a reduced binocular overlap in the anterior sagittal plane compared to the chicken and quail.

The peafowl retina also displays a weakly defined visual streak extending horizontally from the area centralis. Visual streaks are common in mammals (Hughes, 1977) and birds (Hayes and Brooke, 1990; Meyer, 1977) that inhabit open environments where the visual horizon is largely unrestricted. In this respect it is interesting to note that the peafowl spends much of its time foraging on open plains and scrubland, whereas the Japanese quail (which is only 17–19 cm tall) prefers dense herbage less than 1 m tall and the red jungle fowl favours the forest understorey (del Hoyo et al., 1994).

Visual resolution

The area centralis is used to view distant objects during monocular fixation, and high spatial resolution is important for both predator and prey detection (Pumphrey, 1948). The calculated visual acuity for the lateral visual field of the peafowl (20.6 cycles degrees^{-1}) is better than that measured behaviourally for the lateral visual field of the pigeon (12.6 cycles degrees^{-1}; Hahmann and Güntürkün, 1993) and the chicken (7.1 cycles degrees^{-1}; see Donner, 1951), largely due to its relatively long PND. Of course, the visual acuity of the peafowl might be considerably poorer if not all of the ganglion cells in the area centralis contribute to spatial tasks. However, estimates of visual acuity made on the basis of anatomy can be remarkably similar to values measured behaviourally: assuming a peak cell density of 31 500 cells mm^{-2} (42 000 cells mm^{-2} corrected for 25% shrinkage) in the area centralis of the pigeon (Binggeli and Paule, 1969) and that about 85% of these are ganglion cells (Hayes, 1984), and a PND of 7.9 mm (Marshall et al., 1973), the calculated maximum visual acuity in the lateral visual field of the pigeon would be 12.1 cycles degrees^{-1} (see also Wathey and Pettigrew, 1989).

Abbreviations

LWS	long wavelength sensitive
MSP	microspectrophotometer
MWS	medium wavelength sensitive
PBS	phosphate-buffered saline
PND	posterior nodal distance
SWS	short wavelength sensitive
UVS	ultraviolet sensitive
VS	violet sensitive
λ_{cut}	cut-off wavelength
λ_{max}	wavelength of maximum absorbance
λ_{mid}	wavelength of half maximum-measured absorptance
$\lambda T_{0.5}$	wavelength of 0.5 transmittance

The author would like to thank Justin Marshall, Misha Vorobyev and David Vaney for useful discussions. The work was partly funded by the BBSRC (Research Studentship 95/RS/ASP/099 to N.S.H. and Research grant 7/S05042 to Innes C. Cuthill and Julian C. Partridge) at the University of Bristol, UK, where most of the work was conducted, and also by a University of Queensland Postdoctoral Research Fellowship to N.S.H. All experiments complied with the 'Principals of Animal Care', publication No. 86-23, revised 1985, of the National Institute of Health.

References

Ahnelt, P. K. and Kolb, H. (2000). The mammalian photoreceptor mosaic – adaptive design. *Prog. Retin. Eye Res.* **19**, 711-777.

Barlow, H. B. (1982). What causes trichromacy? A theoretical analysis using comb-filtered spectra. *Vision Res.* **22**, 635-643.

Bennett, A. T. D., Cuthill, I. C. and Norris, K. J. (1994). Sexual selection and the mismeasure of color. *Am. Nat.* **144**, 848-860.

Binggeli, R. L. and Paule, W. J. (1969). The pigeon retina: quantitative aspects of the optic nerve and ganglion cell layer. *J. Comp. Neurol.* **137**, 1-18.

Bowmaker, J. K. (1977). The visual pigments, oil droplets and spectral sensitivity of the pigeon. *Vision Res.* **17**, 1129-1138.

Bowmaker, J. K., Heath, L. A., Wilkie, S. E. and Hunt, D. M. (1997). Visual pigments and oil droplets from six classes of photoreceptor in the retinas of birds. *Vision Res.* **37**, 2183-2194.

Bowmaker, J. K., Kovach, J. K., Whitmore, A. V. and Loew, E. R. (1993). Visual pigments and oil droplets in genetically manipulated and carotenoid deprived quail: a microspectrophotometric study. *Vision Res.* **33**, 571-578.

Budnik, V., Mpodozis, J., Varela, F. J. and Maturana, H. R. (1984). Regional specialization of the quail retina: ganglion cell density and oil droplet distribution. *Neurosci. Lett.* **51**, 145-150.

Chen, Y. and Naito, J. (1999). A quantitative analysis of cells in the ganglion cell layer of the chick retina. *Brain Behav. Evol.* **53**, 75-86.

Collin, S. P. and Pettigrew, J. D. (1989). Quantitative comparison of the limits on visual spatial resolution set by the ganglion cell layer in twelve species of reef teleosts. *Brain Behav. Evol.* **34**, 184-192.

del Hoyo, J., Elliot, A. and Sargatal, J. (1994). *Handbook of the Birds of the World*. Vol. 2. *New World Vultures to Guineafowl*. Barcelona: Lynx Edicions.

Delius, J. D. and Emmerton, J. (1979). Visual performance of pigeons. In *Neural Mechanisms of Behaviour in the Pigeon* (ed. A. M. Granda and J. H. Maxwell), pp. 51-69. New York: Plenum Press.

Donner, K. O. (1951). The visual acuity of some passerine birds. *Acta Zool. Fenn.* **66**, 1-40.

Ehrlich, D. (1981). Regional specialization of the chick retina as revealed by the size and density of neurons in the ganglion cell layer. *J. Comp. Neurol.* **195**, 643-657.

Govardovskii, V. I. (1983). On the role of oil drops in colour vision. *Vision Res.* **23**, 1739-1740.

Govardovskii, V. I., Fyhrquist, N., Reuter, T., Kuzmin, D. G. and Donner, K. (2000). In search of the visual pigment template. *Vis. Neurosci.* **17**, 509-528.

Hahmann, U. and Güntürkün, O. (1993). The visual acuity for the lateral visual field of the pigeon (*Columba livia*). *Vision Res.* **33**, 1659-1664.

Hart, N. S. (2001a). Variations in cone photoreceptor abundance and the visual ecology of birds. *J. Comp. Physiol. A* **187**, 685-697.

Hart, N. S. (2001b). The visual ecology of avian photoreceptors. *Prog. Retin. Eye Res.* **20**, 675-703.

Hart, N. S., Partridge, J. C., Bennett, A. T. D. and Cuthill, I. C. (2000a). Visual pigments, cone oil droplets and ocular media in four species of estrildid finch. *J. Comp. Physiol. A* **186**, 681-694.

Hart, N. S., Partridge, J. C. and Cuthill, I. C. (1998). Visual pigments, oil droplets and cone photoreceptor distribution in the European starling (*Sturnus vulgaris*). *J. Exp. Biol.* **201**, 1433-1446.

Hart, N. S., Partridge, J. C. and Cuthill, I. C. (1999). Visual pigments, cone oil droplets, ocular media and predicted spectral sensitivity in the domestic turkey (*Meleagris gallopavo*). *Vision Res.* **39**, 3321-3328.

Hart, N. S., Partridge, J. C. and Cuthill, I. C. (2000b). Retinal asymmetry in birds. *Curr. Biol.* **10**, 115-117.

Hart, N. S., Partridge, J. C., Cuthill, I. C. and Bennett, A. T. D. (2000c). Visual pigments, oil droplets, ocular media and cone photoreceptor distribution in two species of passerine bird: the blue tit (*Parus caeruleus* L.) and the blackbird (*Turdus merula* L.). *J. Comp. Physiol. A* **186**, 375-387.

Hayes, B., Martin, G. R. and Brooke, M. d. L. (1991). Novel area serving binocular vision in the retinae of procellariiform seabirds. *Brain Behav. Evol.* **37**, 79-84.

Hayes, B. P. (1984). Cell populations of the ganglion cell layer: displaced amacrine and matching amacrine cells in the pigeon retina. *Exp. Brain Res.* **56**, 565-573.

Hayes, B. P. and Brooke, M. d. L. (1990). Retinal ganglion cell distribution and behaviour in procellariform seabirds. *Vision Res.* **30**, 1277-1289.

Hughes, A. (1977). The topography of vision in mammals of contrasting life styles: comparative optics and retinal organisation. In *The Visual System in Vertebrates*, vol. VII/5 (ed. F. Crescitelli), pp. 613-756. Berlin: Springer-Verlag.

Inzunza, O., Bravo, H., Smith, R. L. and Angel, M. (1991). Topography and morphology of retinal ganglion cells in *Falconiforms*: a study on predatory and carrion-eating birds. *Anat. Rec.* **229**, 271-277.

Jacobs, G. H. (1981). *Comparative Color Vision*. New York, London: Academic Press.

Jane, S. D. and Bowmaker, J. K. (1988). Tetrachromatic colour vision in the duck (*Anas platyrhynchos* L.): microspectrophotometry of visual pigments and oil droplets. *J. Comp. Physiol. A* **162**, 225-235.

Levine, J. S. and MacNichol, E. F., Jr (1985). Microspectrophotometry of primate photoreceptors: art, artefact and analysis. In *The Visual System* (ed. A. Fein and J. S. Levine), pp. 73-87. New York: Liss.

Lipetz, L. E. (1984). A new method for determining peak absorbance of dense pigment samples and its application to the cone oil droplets of *Emydoidea blandingii*. *Vision Res.* **24**, 597-604.

Lythgoe, J. N. (1979). *The Ecology of Vision*. Oxford: Oxford University Press.

MacNichol, E. F., Jr (1986). A unifying presentation of photopigment spectra. *Vision Res.* **26**, 1543-1556.

Marshall, J., Mellerio, J. and Palmer, D. A. (1973). A schematic eye for the pigeon. *Vision Res.* **13**, 2449-2453.

Martin, G. R. (1985). *Eye*, vol. 3 (ed. A. S. King and J. McLelland), pp. 311-373. London: Academic Press.

Martin, G. R. (1986). The eye of a passeriform bird, the European starling (*Sturnus vulgaris*): eye movement amplitude, visual fields and schematic optics. *J. Comp. Physiol. A* **159**, 545-557.

Meyer, D. B. (1977). The avian eye and its adaptations. In *The Visual System in Vertebrates*, vol. VII/5 (ed. F. Crescitelli), pp. 549-611. Berlin: Springer-Verlag.

Moroney, M. K. and Pettigrew, J. D. (1987). Some observations on the visual optics of kingfishers (Aves, Coraciformes, Alcedinidae). *J. Comp. Physiol. A* **160**, 137-149.

Morris, V. B. and Shorey, C. D. (1967). An electron microscope study of types of receptor in the chick retina. *J. Comp. Neurol.* **129**, 313-340.

Nalbach, H.-O., Wolf-Oberhollenzer, F. and Remy, M. (1993). Exploring the image. In *Vision, Brain and Behavior in Birds* (ed. H. P. Zeigler and H.-J. Bischof), pp. 25-46. Cambridge, Massachussets: MIT Press.

Parrish, J., Benjamin, R. and Smith, R. (1981). Near-ultraviolet light reception in the mallard. *Auk* **98**, 627-628.

Partridge, J. C. (1989). The visual ecology of avian cone oil droplets. *J. Comp. Physiol. A* **165**, 415-426.

Petrie, M. (1994). Improved growth and survival of offspring of peacocks with more elaborate trains. *Nature* **371**, 598-599.

Petrie, M. and Halliday, T. (1994). Experimental and natural changes in the peacock's (*Pavo cristatus*) train can affect mating success. *Behav. Ecol. Sociobiol.* **35**, 213-217.

Petrie, M. and Williams, A. (1993). Peahens lay more eggs for peacocks with larger trains. *Proc. R. Soc. Lond. B* **251**, 127-131.

Pettigrew, J. D., Dreher, B., Hopkins, C. S., McCall, M. J. and Brown, M. (1988). Peak density and distribution of ganglion cells in the retinae of Microchiropteran bats: implications for visual acuity. *Brain Behav. Evol.* **32**, 39-56.

Pumphrey, R. J. (1948). The sense organs of birds. *Ibis* **90**, 171-199.

Schaeffel, F. and Howland, H. C. (1988). Visual optics in normal and ametropic chickens. *Clin. Vision Sci.* **3**, 83-98.

Sibley, C. G. and Monroe, B. L., Jr (1990). *Distribution and Taxonomy of Birds of the World*. New Haven: Yale University Press.

Snyder, A. W. and Miller, W. H. (1977). Photoreceptor diameter and spacing for highest resolving power. *J. Opt. Soc. Am.* **67**, 696-698.

Stone, J. (1981). *The Whole Mount Handbook*. Sydney: Maitland Publications Pty. Ltd.

Vorobyev, M., Marshall, J., Osorio, D., Hempel de Ilbarra, N. and Menzel, R. (2001). Colourful objects through animal eyes. *Color Res. Appl.* **26**, S214-217.

Vorobyev, M. and Osorio, D. (1998). Receptor noise as a determinant of colour thresholds. *Proc. R. Soc. Lond. B* **265**, 351-358.

Vorobyev, M., Osorio, D., Bennett, A. T. D., Marshall, N. J. and Cuthill, I. C. (1998). Tetrachromacy, oil droplets and bird plumage colours. *J. Comp. Physiol. A* **183**, 621-633.

Wathey, J. C. and Pettigrew, J. D. (1989). Quantitative analysis of the retinal ganglion cell layer and optic nerve of the barn owl *Tyto alba*. *Brain Behav. Evol.* **33**, 279-292.

Wood, C. A. (1917). *The Fundus Oculi of Birds Especially as Viewed by the Ophthalmoscope.* Chicago: Lakeside Press.